Modeling of Independent Energy Communities Sharing the Same Distribution Network

Published Version:
Harighi, T., Lilla, S., Borghetti, A. (2024). Modeling of Independent Energy Communities Sharing the Same Distribution Network. 345 E 47TH ST, NEW YORK, NY 10017 USA : Institute of Electrical and Electronics Engineers Inc. [10.1109/SEST61601.2024.10694676].

Availability:
This version is available at: https://hdl.handle.net/11585/1001212 since: 2025-01-27

Published:
DOI: http://doi.org/10.1109/SEST61601.2024.10694676

(Article begins on next page)

Modeling of Independent Energy Communities Sharing the Same Distribution Network

Tohid Harighi, Stefano Lilla, and Alberto Borghetti
University of Bologna
Bologna, Italy
{tohid.harighi2, stefano.lilla3, alberto.borghetti}@unibo.it

***Abstract*—Recent regulatory frameworks in several countries are introducing energy communities, which are collectives of prosumers and users that exchange active power while maintaining independence. Users are free to join or not, and to choose their electricity retailer. This paper considers the presence of multiple communities in the same distribution network (as allowed by regulation) and presents a model that independently optimize the operation of each community and manages network constraints. The price of the energy transactions between community members are determined as shadow prices of balancing constraints. Day-ahead scheduling results are presented for different community configurations and data sets from a real 15 kV distribution network. The paper analyzes the electricity procurement costs of both community members and non-members. The results show the effectiveness in reducing both energy procurement costs and noncompliance costs for each community. The sensitivity analysis on the number of ECs shows that as the number of ECs increases, cost reductions and penalties decrease, approaching the case without internal transactions within ECs.**

***Index Terms*—Energy community optimization, Distribution systems, Active and reactive power exchanges, Network constraints, Shadow pricing.**

NOMENCLATURE

OF^{c} Objective function for community c
OF^{DSO} DSO objective function
N Number of buses on the distribution network
M Large number to differentiate violations in DSO model
$pf_{\min}$, μ_{PF} Minimum power factor to avoid penalty, noncompliance penalty rate
V_0 Voltage at the transmission grid connection point
For user i of community c at time t
C_{fossil} Fossil fuel unit operating costs
$\pi_{\mathrm{buy/sell}}$ Reseller buying/selling tariffs
$P_{\mathrm{L/G/BES}}$ Active power of local load/generation/BES system
$Q_{\mathrm{L/G/BES/C}}$ Reactive power of local load/generation/BES system/capacitor bank
C_{grid} Costs/revenues for energy bought from/sold to retailer
$Q_{\mathrm{PF}\ i,t}$ Excess reactive power
P_{LEC}, Q_{LEC} Active and reactive power exchanges within EC
P_{grid}, Q_{grid} Active and reactive power exchanges with retailer
P_{user}, Q_{user} Active and reactive net power
ℓ_{BES}, $\eta_{\mathrm{charge/discharge}}$ BES losses, charge/discharge efficiency
E, $E_{\mathrm{min/max}}$ BES stored energy, minimum/maximum limits
Q_{PF}, $Q_{\lim 1/2}$, $\hat{Q}$ Reactive power excess, minimum pf limits, sum of controllable reactive power resources
For node/branch k of the network at time t
$I_{\max}$, $\Delta u_{\mathrm{in/out}}$ Max. branch current, square current violation
r, x, b, t_{OLTC} Longitudinal resistance, reactance, shunt susceptance, and transformer ratio of the branch model
$V_{\mathrm{min/max}}$, $\Delta v_{\mathrm{min/max}}$ Minimum/maximum bus voltage limits, minimum/maximum square voltage violation
v Square rms value of bus voltage
$v_{\mathrm{in/out/mp}}$ Input/output/central node square voltage
v'_{out} Square voltage at the ideal transformer primary side
$u_{\mathrm{in/out}}$ Input/output branch square voltage
$P_{\mathrm{in/out/mp}}$ Input/output/central node active power
$Q_{\mathrm{in/out/mp}}$ Input/output/central node reactive power
For users connected to node k at time t
P^{c}, Q^{c} Bus active/reactive power relevant to community c
$\lambda^{\mathrm{uP/vP}}$ P multipliers to limit current/voltage violations
$\lambda^{\mathrm{uQ/vQ}}$ Q multipliers to limit current/voltage violations
$\mu^{\mathrm{P/Q}}$ Shadow prices of the P/Q constraints at each node
Sets
T Optimization horizon of periods t
Ω_c, noEC Users in community c or outside communities
Ω_c^k Users of community c supplied by bus k
Θ_k Subset of Ω_c served by the same transformer
$\Omega_j^{\mathrm{in/out}}$ Branches connected to bus j at send/receive end

I. INTRODUCTION

The development of Energy Communities (ECs) of prosumers, facilitated by the evolving regulatory framework, e.g., in Europe [1], is expected to facilitate a further integration of renewable energy sources and the installation of energy storage systems in distribution networks [2].

There is a growing literature on modeling of energy communities and optimal scheduling of the exchanges among their members, taking explicitly into account the limits due to the technical characteristics of the power distribution network. Local market structures are described, for example, in [3]-[7] and references therein. Specifically, the model proposed in [3] takes into account the network constraints by including three factors in the market mechanism: voltage sensitivity coefficients, power transfer distribution factors, loss sensitivity factors. In [4], the proposed peer-to-peer (P2P) platform is based on the use of locational marginal prices to calculate network usage charges. In [5] an approach is proposed consisting of three layers: the market layer sending price signals to the EC controller layer, the controller layer for managing the energy flow, and the grid layer for studying the impact on the distribution grid. A Stackelberg-game framework is adopted in [6] to set prices by the distribution system operator (DSO). The focus is the optimal operation of distribution networks that incorporate ECs, by adopting a bi-level optimization scheme. The pricing scheme proposed in [8] addresses the challenges of energy trading in a local electricity market through a decision-making process that includes look-ahead energy storage scheduling. The hosting capacity of a distribution network in presence of ECs is analyzed in [7] by using Monte Carlo simulations for the entire year in order to represent different EC configurations and the effects on energy losses, bus voltage deviations, and thermal loading of branches. The impact on the medium voltage (MV) network is reduced when the EC is operated to minimize the power exchange between the EC and the external grid for each individual time stamp.

Compared to earlier studies, this paper focuses on the analysis of the presence of multiple ECs, with members served by different electricity retailers, in the MV power distribution network. The analysis is carried out by a specifically developed procedure that provides the daily optimization of the communities that consider direct transactions of both active and reactive power between their members and helps in solving network congestions. In this approach, each community minimizes its energy procurement costs through a day-ahead scheduling of internal transactions among its members and available energy resources, including battery energy storage (BES) systems. Members of the same community may be served by different electricity retailers. Each retailer has different contract terms. Internal transactions are priced using the shadow prices of the balancing constraints between the power provided by the electricity retailer and the power received by other community members.

Preliminary results using the IEEE 123-bus feeder test system and a centralized optimization approach have been presented in [9]. This paper extends the model by representing the use of reactive energy exchanges among members of each EC to limit the penalties due to minimum power factor (PF) operations and by adopting an iterative distributed optimization procedure based on the augmented Lagrangian method [10] to take into account violations of network constraints. Specifically, the objective function of the optimization of each EC is augmented by the penalization coefficients updated at each iteration to minimize the violations of both bus voltage and branch current limits, using a typical sensitivity estimation [11].

The paper presents the results for different numbers and configurations of communities, price profiles of electricity retailers, and network operating constraints. The paper also shows the computational feasibility of the proposed approach.

II. Day-ahead Distributed Optimization Procedure

The procedure focuses on the day-ahead optimization for the next 24 hours, divided into 96 periods of 15 minutes each. The optimization independently performed for each community and the set of users outside the communities, called noEC, with the goal of minimizing the corresponding energy supply costs. In addition, there is an optimization problem for the DSO, which takes into account the network constraints and minimizes the violations of the limits of the branch currents and the bus voltages. The procedure is iterative and stops when the violations of the network constraints in the DSO problem are less than a predefined tolerance or when there are no more improvements to the solution.

The next two subsections describe in detail the models implemented for the communities, the noEC set of users, and the DSO problem.

A. Individual and Collective User Optimization Model

The model is a mixed-integer linear programming problem. To obtain the day-ahead scheduling of the available energy resources and of the transactions between the members of the same community, the following objective function is minimized:

$$\begin{aligned} OF^{\mathrm{c}} = \sum_{t\in T} \Bigg\{ & \sum_{i\in\Omega_c} \left(C_{\mathrm{fossil}\,i,t} + C_{\mathrm{grid}\,i,t} + \mu_{\mathrm{PF}}\; Q_{\mathrm{PF}\,i,t}\right)\Delta t \\ & + \sum_{k=1}^{N} \left[\left(\lambda^{\mathrm{uP}}_{k,t} + \lambda^{\mathrm{vP}}_{k,t}\right) P^{c}_{k,t} + \left(\lambda^{\mathrm{uQ}}_{k,t} + \lambda^{\mathrm{vQ}}_{k,t}\right) Q^{c}_{k,t} \right] \Bigg\} \end{aligned} \tag{1}$$

which includes the operating costs, the penalization for the low PF operation and the additional terms useful to limit the network constraint violations. Multipliers λ are provided by the DSO model at each iteration. The noncompliance amount $Q_{\mathrm{PF}\,i,t}$ is the excess reactive power with respect $pf_{\min}$. The value of μ_{PF} is assumed to be known, i.e. set by the regulator or utility.

$C_{\mathrm{grid}\,i,t}$ is constrained by:

$$C_{\mathrm{grid}\,i,t} \geq \pi_{\mathrm{buy}\,i,t} P_{\mathrm{grid}\,i,t} \quad C_{\mathrm{grid}\,i,t} \geq \pi_{\mathrm{sell}\,i,t} P_{\mathrm{grid}\,i,t} \tag{2}$$

where $P_{\mathrm{grid}\,i,t}$ is positive when bought and negative otherwise.

Contributions $P^{c}_{k,t}$ and $Q^{c}_{k,t}$ to the power at node k of the network are:

$$P^{c}_{k,t} = \sum_{i\in\Omega^{k}_{c}} P_{\mathrm{user}\,i,t} \quad Q^{c}_{k,t} = \sum_{i\in\Omega^{k}_{c}} Q_{\mathrm{user}\,i,t} \tag{3}$$

Following the approach presented in [9], the total net consumption (positive) or production (negative) of user i should balance the sum of the exchanges with the retailer and with the other members of the same community c:

$$P_{\mathrm{user}\,i,t} = P_{\mathrm{grid}\,i,t} + P_{\mathrm{LEC}\,i,t} \tag{4}$$

Constraint (4) is associated with the condition that the sign of $P_{\mathrm{user}\,i,t}$ $P_{\mathrm{grid}\,i,t}$ and $P_{\mathrm{LEC}\,i,t}$ is the same (dealt with the inclusion of binary variables associated with the sign of $P_{\mathrm{user}\,i,t}$). The prices of the P_{LEC} transactions between the community members are calculated as the shadow prices of constraint (4).

As $Q_{\mathrm{grid}\,i,t}$ is typically constrained to be nonnegative:

$$Q_{\mathrm{user}\,i,t} = \begin{cases} Q_{\mathrm{grid}\,i,t} + Q_{\mathrm{LEC}\,i,t} & \text{if } Q_{\mathrm{user}\,i,t} \geq 0, \\ Q_{\mathrm{LEC}\,i,t} & \text{if } Q_{\mathrm{user}\,i,t} < 0. \end{cases} \tag{5}$$

The condition on the sign of $Q_{\text{user}\,i,t}$ (positive if consumed) is dealt with through specific binary variables.

For the users of set noEC, the only difference with respect to the community model is that the exchange between users is prohibited, i.e. $P_{\text{LEC}\,i,t} = 0$ and $Q_{\text{LEC}\,i,t} = 0$ if i in noEC.

The exchange between the members of each community Ω_k is balanced and the reactive power exchange is limited to the members of the community that are served by the same HV/MV transformer:

$$\sum_{i \in \Omega_c} P_{\text{LEC}\,i,t} = 0 \quad \sum_{i \in \Theta_k} Q_{\text{LEC}\,i,t} = 0 \tag{6}$$

The net power for each user is given by:

$$\begin{aligned} P_{\text{user}\,i,t} &= P_{\text{L}\,i,t} - P_{\text{G}\,i,t} - P_{\text{BES}\,i,t} + \ell_{\text{BES}\,i,t} \\ Q_{\text{user}\,i,t} &= Q_{\text{L}\,i,t} - Q_{\text{G}\,i,t} - Q_{\text{BES}\,i,t} - Q_{\text{C}\,i,t} \end{aligned} \tag{7}$$

Q_G, Q_{BES} are limited by the minimum PF of the local generator and the BES. Q_{C} is fixed or limited by the maximum power of the switchable capacitor bank (discrete switching is not represented for simplicity). P_{BES} is positive when the battery is discharged and is constrained by the maximum power limit of the battery system.

BES power losses $\ell_{\text{BES}\,i,t}$ are

$$\ell_{\text{BES}\,i,t} = \begin{cases} (1 - \eta_{\text{discharge}\,i}) P_{\text{BES}\,i,t} & \text{if } P_{\text{BES}\,i,t} \geq 0 \\ (1 - 1/\eta_{\text{charge}\,i}) P_{\text{BES}\,i,t} & \text{if } P_{\text{BES}\,i,t} < 0 \end{cases} \tag{8}$$

where the condition on the sign of $P_{\text{BES}\,i,t}$ is treated with a specific binary variable. The model of the BES unit is given by:

$$\begin{aligned} &E_{i,t} = E_{i,t-1} - P_{\text{BES}\,i,t}\,\Delta t \text{ for } 1 < t < 96 \\ &E_{i,1} = E_{\max i} - P_{\text{BES}\,i,1}\,\Delta t \quad \text{and } E_{i,96} = E_{\max i} \end{aligned} \tag{9}$$

By defining $\hat{Q}_{\,i,t} = Q_{\text{G}\,i,t} + Q_{\text{C}\,i,t} + Q_{\text{BES}\,i,t} + Q_{\text{LEC}\,i,t}$, if the operating condition is not satisfying $pf_{\min}$, a penalty is applied in (1) proportional to the amount of reactive power excess, denoted as $Q_{\text{PF}\,i,t}$:

$$Q_{\text{PF}\,i,t} \geq \begin{cases} \operatorname{sgn}(P_{\text{user}\,i,t}) \left(Q_{\lim 1\,i,t} - \hat{Q}_{i,t} \right) \\ \operatorname{sgn}(P_{\text{user}\,i,t}) \left(\hat{Q}_{i,t} - Q_{\lim 2\,i,t} \right) \end{cases} \tag{10}$$

where

$$\begin{aligned} Q_{\lim 1\,i,t} &= Q_{\text{L}\,i,t} - \tan\left(\arccos pf_{\min}\right) P_{\text{user}\,i,t} \\ Q_{\lim 2\,i,t} &= Q_{\text{L}\,i,t} + \tan\left(\arccos pf_{\min}\right) P_{\text{user}\,i,t} \end{aligned} \tag{11}$$

B. DSO Model

The DSO problem minimizes the violations of the network constraints in both bus voltages and branch currents.

The configuration of the MV network is radial, so excluding the slack bus, which is the substation HV bus, the number of nodes is equal to the number of buses. A common index k is used to denote both a branch and the corresponding end.

The model of the network represents each branch with a balanced T-model, composed of two impedances (called in and out) each equal to half the longitudinal impedance of the branch and a shunt admittance in the middle (Fig. 1).

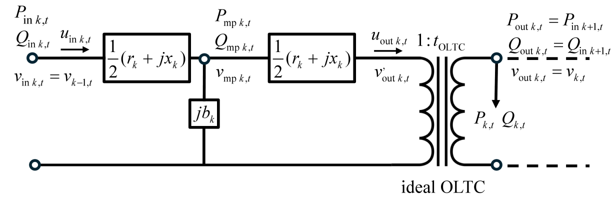

Fig. 1. Generic T-model equivalent circuit

The model adopts the DistFlow approach [12], which uses the square rms values of the input and output currents $u_{\text{in}\,k,t}$ and $u_{\text{out}\,k,t}$, respectively, and the square rms values of the bus voltages, $v_{k,t}$. The nonnegative violations are:

$$\begin{aligned} &\Delta u_{\text{in}\,k,t} \geq u_{\text{in}\,k,t} - I^2_{\max k}, \;\; \Delta u_{\text{out}\,k,t} \geq u_{\text{out}\,k,t} - I^2_{\max k} \\ &\Delta v_{\min k,t} \geq V^2_{\min k} - v_{k,t}, \;\; \Delta v_{\max k,t} \geq v_{k,t} - V^2_{\max k} \end{aligned} \tag{12}$$

By defining $\Delta u_t = \sum_{k=1}^{N} (\Delta u_{\text{in}\,k,t} + \Delta u_{\text{out}\,k,t})$ and $\Delta v_t = \sum_{k=1}^{N} (\Delta v_{\min\,k,t} + \Delta v_{\max\,k,t})$, the DSO problem minimizes the summation of the violations:

$$OF^{\text{DSO}} = \sum_{t \in T} (\Delta u_t + M\,\Delta v_t) \tag{13}$$

where M differentiates the maximum branch current violations from the bus voltage violations.

The application of the balanced DistFlow linearization presented in [13] to the T-model equations described in [14] yields, for each branch k, the relationships that relate the square rms values of the voltages with the power flows are:

$$\begin{aligned} v_{\text{mp}\,k,t} &= v_{\text{in}\,k,t} - r_k P_{\text{in}\,k,t} - x_i Q_{\text{in}\,k,t} + \tfrac{1}{4}(r_k^2 + x_k^2) u_{\text{in}\,k,t} \\ v_{\text{in}\,k,t} - v'_{\text{out}\,k,t} &= 2 r_k P_{\text{in}\,k,t} + 2 x_k Q_{\text{in}\,k,t} + x_k b_k v_{\text{mp}\,k,t} \\ &\quad - \tfrac{3}{4}(r_k^2 + x_k^2) u_{\text{in}\,k,t} - \tfrac{1}{4}(r_k^2 + x_k^2) u_{\text{out}\,k,t} \end{aligned} \tag{14}$$

where $P_{\text{in}\,k,t} = P_{\text{out}\,k,t} + P_{\text{user}\,k,t} + \frac{1}{2}\, r_k u_{\text{in}\,k,t} + \frac{1}{2}\, r_k u_{\text{out}\,k,t}$, $Q_{\text{in}\,k,t} = Q_{\text{out}\,k,t} + Q_{\text{user}\,k,t} - b_k v_{\text{mp}\,k,t} + \frac{1}{2}\, x_k u_{\text{in}\,k,t} + \frac{1}{2}\, x_k u_{\text{out}\,k,t}$.

The linear representation of the branch currents is

$$\begin{aligned} u_{\text{in}\,k,t} &= 2\,P^0_{\text{ini}\,k,t}\,P_{\text{in}\,i,t} + 2\,Q^0_{\text{ini}\,k,t}\,Q_{\text{ini}\,k,t} \\ &\qquad - \left[(P^0_{\text{ini}\,k,t})^2 + (Q^0_{\text{ini}\,k,t})^2 \right] \\ u_{\text{out}\,k,t} &= 2\,P^0_{\text{mp}\,k,t}\,P_{\text{mp}\,i,t} + 2\,Q^0_{\text{mp}\,k,t}\,Q_{\text{mp}\,k,t} \\ &\qquad - \left[(P^0_{\text{mp}\,k,t})^2 + (Q^0_{\text{mp}\,k,t})^2 \right] \end{aligned} \tag{15}$$

that uses the power flow estimate marked with superscript 0, calculated by building the set of all buses that each branch feeds and then by adding the corresponding bus power, assuming bus voltages equal to 1 pu, as well as neglecting the control of on-load tap changers (OLTC), batteries, capacitor banks, and dispatchable generators.

The substation transformers have $v_{\text{in}\,k,t} = V_0^2$, assumed to be known and constant throughout the day. They are OLTC equipped with a tap ratio in the range $[t_{\min}, t_{\max}]$, continuous for simplicity, so that:

$$v_{\text{out}\,k,t} \leq t^2_{\max}\, v'_{\text{out}\,k,t} \quad \text{and} \quad v_{\text{out}\,k,t} \geq t^2_{\min}\, v'_{\text{out}\,k,t} \tag{16}$$

For all the branches that do not represent an OLTC transformer $v_{\text{out}\,k,t} = v'_{\text{out}\,k,t}$. Generalizing to the case of multiple branches originating and terminating on the same bus, the node equilibrium constraints are:

$$
\begin{aligned}
v_{\text{out}\,k\in\Omega_j^{\text{out}},t} = v_{\text{in}\,k\in\Omega_j^{\text{in}},t} &= v_{k,t} \\
\sum_{k\in\Omega_j^{\text{out}}} P_{\text{out}\,k,t} &= \sum_{k\in\Omega_j^{\text{in}}} P_{\text{in}\,k,t} \\
\sum_{k\in\Omega_j^{\text{out}}} Q_{\text{out}\,k,t} &= \sum_{k\in\Omega_j^{\text{in}}} Q_{\text{in}\,k,t}
\end{aligned}
\tag{17}
$$

The values of the power at each bus are given by the solution of the optimization problem for each community and the users outside the community, as defined by (3). The summation gives the total power at each bus of the network:

$$
P_{k,t} = \sum_c P^c_{k,t} \;\; : \mu^{\text{P}}_{k,t} \qquad Q_{k,t} = \sum_c Q^c_{k,t} \;\; : \mu^{\text{Q}}_{k,t} \tag{18}
$$

These constraints are associated with the shadow prices that are used to update the multipliers of (1) as described below.

C. Multiplier Update

In each iteration, at first the models of the communities and the noEC users are solved, then the DSO model is solved. Finally, the λ multipliers of the previous iteration, indicated by an upper bar, are updated based on the values of the shadow prices from (18) and the violations from (12):

$$
\lambda^{\text{uP}}_{k,t} = \overline{\lambda}^{\text{uP}}_{k,t} + \widehat{\mu}^{\text{uP}}_{k,t}\Delta u_t \qquad \lambda^{\text{vP}}_{k,t} = \overline{\lambda}^{\text{vP}}_{k,t} + \widehat{\mu}^{\text{vP}}_{k,t}\Delta v_t \tag{19}
$$

and analogously for $\lambda^{\text{uQ}}_{k,t}$ and $\lambda^{\text{vQ}}_{k,t}$.

The shadow prices relevant to current and voltage violations are distinguished in $\mu^{\text{uP}}_{k,t}$, $\mu^{\text{uQ}}_{k,t}$ and $\mu^{\text{vP}}_{k,t}$, $\mu^{\text{vQ}}_{k,t}$ respectively, by comparison with a threshold value set according to the M value introduced in (13). These values are also normalized (indicated by the hat) with respect to the norm of the corresponding prices for all branches and buses.

III. Case Study and Test Results

A. Feeders and User Characteristics

The case study includes 5 real MV feeders (here referred to as A to E) connected to a 132/15 kV substation, located in Modena, Italy (Fig. 2). The substation is equipped with a 50 MVA transformer (T1) and two 25 MVA transformers (T2 and T3), all with OLTCs. The system includes 134 buses and branches: 4 in feeder A connected to transformer T2, 27 in feeder B connected to transformer T1, 22 in feeder C connected to transformer T1, 26 in feeder D connected to transformer T1, and 55 in feeder E connected to transformer T3.

Three electricity retailers (Pr1, Pr2, and Pr3) with different price profiles are considered: one (with minimum and maximum values equal to 0.093 €/kWh and 0.33 €/kWh, respectively) follows the typical wholesale market price behavior with two peaks in the morning (9-11 am) and in the evening (6-9 pm), the second profile (with the same maximum and minimum values) has a low price during the night and a higher price during the day, the third is a 10% discount with respect to the second one. The π_{sell} profiles follow similar patterns, but with values halved.

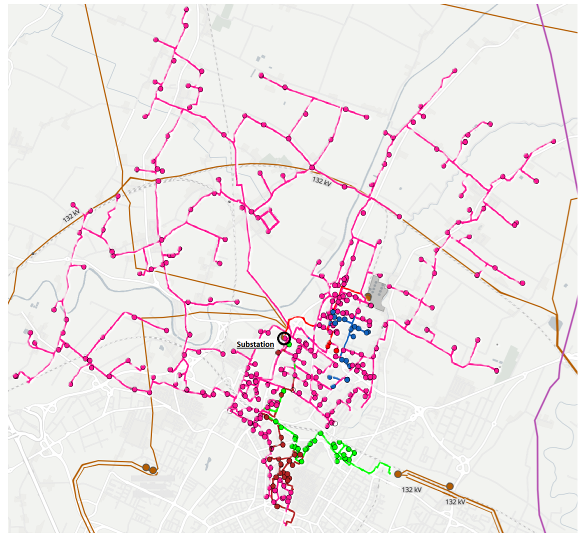

Fig. 2. Layout of the real MV test network. The HV/MV substation is indicated by a circle and, the five feeders considered are distinguished by different colors.

For illustrative purposes, μ_{PF} is assumed to be equal to 5 €/kvarh. The requested pf_{min} value is assumed to be 0.9. The bus voltage values are constrained to be within the interval 0.9 pu - 1.1 pu.

The load and generation profiles are obtained from the DSO records at each 15-minute interval, separately for each MV node, for three days in January and in July, 2023. The weather data are summarized in Table I [15].

TABLE I
WEATHER DATA

	Winter (January)			Summer (July)		
Property	17	18	19	18	19	20
Cloud Coverage (%)	88.1	84.1	85.5	11	25.2	34.1
Solar Radiation (W/m^2)	8	40	13	296	264	303
Temperature (°C)	4.1	3.8	2.6	30.2	30.2	27.4
Wind Speed (km/h)	37.1	13.2	17.1	14.8	18.4	20.5
Precipitations (mm)	3.1	0.2	3.2	0	0	2.6

The data of daily load consumption, PV generation and the generation from synchronous machines are summarized in Table II. The voltage dependence of the loads is neglected. The users have batteries with a total capacity of 675 kWh.

TABLE II
ENERGY CONSUMPTION AND GENERATION DATA

	Winter (January)			Summer (July)		
Property	17	18	19	18	19	20
Load Consumption (MWh)	267.9	277.6	269.1	327.8	333.0	320.5
PV Generation (MWh)	5.8	6.2	6.0	11.0	10.6	11.0
in % wrt to Consumption	2.16	2.23	2.22	3.35	3.18	3.43
Sync. Generation (MWh)	11.4	11.4	10.6	11.5	11.5	11.5

Each user is randomly assigned to one of the three retailers. Similarly, users are randomly grouped, with equal probability, into three communities (EC1, EC2, EC3), or are not included in any community (noEC set). For the sake of simplicity, all the users connected to the same MV node are considered to be aggregated, and thus to belong to the same community or to the noEC set. Table III shows the allocation of the total energy demand during the three days, the corresponding PV generation, and the total installed storage capacity.

The test case data are available in an Excel file at [16].

The next subsection presents the results for the three community configuration described above, referred to as the base case. Then, the results are compared with the cases where Q_{LEC} and also P_{LEC} transactions are forbidden, and with cases characterized by different numbers of communities. All the results are obtained by implementing of the optimization procedure in AIMMS with the Gurobi solver. The total computational time for each case is less than 2 minutes (CPU: Intel core i7, 12700H 5.2Ghz, RAM: 32GB).

TABLE III
ALLOCATION OF THE DEMAND, PV GENERATION, AND BATTERY STORAGE AS PERCENTAGE OF THE TOTAL THREE-DAY VALUES FOR THE COMMUNITIES AND THE NOEC SET

Group	Demand (%)		Generation (%)		Installed BES (%)
	Winter	Summer	Winter	Summer	
EC1	26.3	27.2	37.2	33.6	14.8
EC2	15.5	14.1	5.4	14.2	44.4
EC3	25.3	27.0	17.2	11.5	14.8
noEC	32.9	31.7	40.2	40.7	26.0

B. Base Case Solution

Table IV shows the cost of the energy provided by the retailers (P_{grid} cost) and the cost due to the internal transactions P_{LEC} (negative values indicate revenues) for the three days in winter and summer for the three communities EC and the three retailers Pr.

TABLE IV
BASE CASE: ENERGY COSTS IN THOUSANDS OF EUROS FOR EACH COMMUNITY CONSIDERING THE THREE DIFFERENT RETAILERS ON WINTER (W) AND SUMMER (S) DAYS

Pr/EC		EC1		EC2		EC3	
	Cost	W	S	W	S	W	S
Pr1	P_{grid}	26.56	31.83	17.62	17.10	30.27	29.63
	P_{LEC}	-1.77	0.16	-0.94	-1.12	-1.72	-0.67
Pr2	P_{grid}	22.93	29.72	10.19	8.21	48.72	71.19
	P_{LEC}	2.83	-0.12	1.05	2.02	1.79	0.67
Pr3	P_{grid}	37.98	43.99	26.97	28.46	11.50	13.82
	P_{LEC}	-1.07	-0.04	-0.11	-0.90	-0.06	0

Table V shows the percentage cost reductions in the base case with respect to the case where both P_{LEC} and Q_{LEC} are prohibited and to the case where only Q_{LEC} transactions are prohibited. The energy costs include both the costs/revenues related to the exchanges with the retailers (P_{grid}) and those related to the exchanges with other community participants (P_{LEC}). The table shows that there are more reductions in winter days than in summer days. In summer, EC2 members also benefit from community participation due to the presence of larger battery storage. Often, users having contracts with Pr1 and Pr2 benefit more from community participation than those with contracts with Pr3, which is the cheapest retailer. The difference between the results obtained in the reference case and those where only Q_{LEC} transactions are prohibited is very small, since the energy costs depend on the active power exchanges.

TABLE V
BASE CASE ENERGY COST REDUCTIONS IN % WITH RESPECT TO THE CASE WHERE P_{LEC} AND Q_{LEC} OR ONLY Q_{LEC} EXCHANGES ARE FORBIDDEN

Pr/EC	forbidded	EC1		EC2		EC3	
		W	S	W	S	W	S
Pr1	$P_{\mathrm{LEC}}/Q_{\mathrm{LEC}}$	5.09	0	2.62	5.22	4.28	1.15
	Q_{LEC}	0	0	0.01	0.05	-0.02	0.22
Pr2	$P_{\mathrm{LEC}}/Q_{\mathrm{LEC}}$	3.34	2.97	0.01	0.04	0	0
	Q_{LEC}	0	0	0	-0.13	0	0
Pr3	$P_{\mathrm{LEC}}/Q_{\mathrm{LEC}}$	1.43	-0.02	0.22	1.24	0.3	0
	Q_{LEC}	0.04	-0.09	0	0.02	0	0

Table VI shows the costs due to minimum PF noncompliance. They are mainly in summer days. The availability of Q_{LEC} transactions is very effective in reducing these costs, as shown by comparing the base case results with those cases where these transactions are forbidden.

TABLE VI
NONCOMPLIANCE COSTS (IN EURO) IN THE BASE CASE AND WHEN P_{LEC} AND Q_{LEC} EXCHANGES ARE FORBIDDEN

	EC1		EC2		EC3	
	W	S	W	S	W	S
Base case	0	12009.2	0.1	0	0	187.5
w/o Q_{LEC}	13.6	33886.7	9.9	5334.8	11.2	15761.6
w/o $P_{\mathrm{LEC}}/Q_{\mathrm{LEC}}$	19.5	33886.7	9.9	5334.8	11.2	15761.6

The goal of reducing the high noncompliance costs may also affect the P_{LEC} transactions. In general, this justifies the reduced benefit on summer days, when the P_{LEC} transactions are limited to reduce noncompliance costs. This also justifies the small negative values in Table V. If Q_{LEC} are forbidden, then the noncompliance cost is high. If P_{LEC} transactions are allowed, the optimization also uses P_{LEC} transactions to reduce the noncompliance cost, and the energy cost may increase slightly compared to the case where transactions are not allowed.

The energy cost values (in thousands of euros) for the users in the noEC group are: in winter days, 19.26, 37.73, 59.15, for the users with contracts with Pr1, Pr2, and Pr3, respectively (total energy cost 116.13); in summer days, 21.54, 40.45, 69.52, for the users with contracts with Pr1, Pr2, and Pr3, respectively (total energy cost 131.52). For the noEC group, in winter days, the the noncompliance cost is €125.1; in summer days, it is €6110.1.

C. Different Number of Communities

For different numbers of communities, Fig. 3 shows the percentage difference in energy procurement and noncompliance costs for users who belong to a community (i.e., those who do not belong to the noEC set in the base case) with respect to the case where P_{LEC} and Q_{LEC} transactions are prohibited. The graphs refer to the three-day costs and penalties, in winter and summer. Without P_{LEC} and Q_{LEC} transactions, the energy procurement and noncompliance costs (in thousands of euros) are 237.3 and 0.034 for winter days, and 276.3 and 55.0 for summer days, respectively.

The figure shows that as the number of communities increase, the percentage reductions decrease, meaning that both costs and penalties approach the values of the case without P_{LEC} and Q_{LEC} transactions.

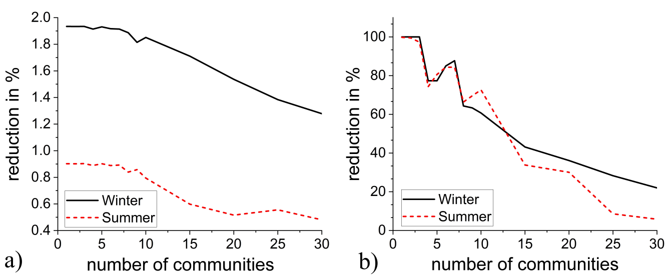

Fig. 3. Percentage reduction of a) energy procurement cost and b) noncompliance penalties, varying the number of communities, with respect to the case in which P_{LEC} and Q_{LEC} transactions are forbidden.

IV. Conclusions

The paper presents a framework for analyzing the effects of multiple energy communities in the same distribution network, while preserving the user's free decision to join or not to join and its autonomous choice of electricity retailer.

The presented day-ahead optimization procedure takes into account the network constraints and provides the prices of the internal transactions as the shadow prices of the power balancing constraints for each user.

In addition, the procedure also allows reactive power exchanges between members of the same community other than active power. These reactive power transactions are performed to reduce the costs for low PF operation.

The procedure is applied to a real MV distribution network, considering the consumption and generation profiles of three days in winter and summer. The results show the effectiveness in reducing both energy procurement costs and noncompliance costs for each community. The sensitivity analysis on the number of ECs shows that as the number of ECs increases, cost reductions and penalties decrease, approaching the case without internal transactions within ECs.

The scheme also appears to be suitable for investigating the provision of flexibility services to the DSO, e.g., for congestion management in the network, as well as the interaction between ECs and transmission network, the effects of the presence ECs on the energy market behavior, and the socio-economic implications for different stakeholders. These aspects are not covered in this paper as they deserve further investigation.

Acknowledgment

The authors would like to thank prof. C.A. Nucci, and the colleagues at Inrete Distribuzione Energia and HERATech (A. Calzolari, M. Salicini, C. Cercolani) for useful support of information, discussions, and comments. The activity has been funded by the Italian Ministry for University and Research through grant J35F21003140006 (PhD program 2014IT16M2OP005), PRIN-2017K4JZEE, and PE0000021 (CUP J33C22002890007).

References

[1] European Union, Models of Local Energy Ownership and the Role of Local Energy Communities in Energy Transition in Europe. 2018.

[2] C. Inês, P. L. Guilherme, M. G. Esther, G. Swantje, H. Stephen, and H. Lars, "Regulatory challenges and opportunities for collective renewable energy prosumers in the EU," Energy Policy, vol. 138, 2020.

[3] J. Guerrero, A. C. Chapman and G. Verbič, "Decentralized P2P energy trading under network constraints in a low-voltage network," in IEEE Transactions on Smart Grid, vol. 10, no. 5, pp. 5163-5173, Sept. 2019, doi: 10.1109/TSG.2018.2878445

[4] J. Kim and Y. Dvorkin, "A P2P-dominant distribution system architecture," in IEEE Trans. on Power Systems, vol. 35, no. 4, pp. 2716-2725, July 2020, doi: 10.1109/TPWRS.2019.2961330.

[5] R. Rana, K. Berg, M. Z. Degefa and M. Löschenbrand, "Modelling and Simulation Approaches for Local Energy Community Integrated Distribution Networks," in IEEE Access, vol. 10, pp. 3775-3789, 2022, doi: 10.1109/ACCESS.2022.3140237.

[6] M. Tostado-Véliz, Y. Liang, A. Rezaee Jordehi, S. A. Mansouri, F. Jurado, "An interval-based bi-level day-ahead scheduling strategy for active distribution networks in the presence of energy communities," in Sustainable Energy, Grids and Networks, vol. 35, 101088:1-16, 2023, doi: 10.1016/j.segan.2023.101088.

[7] A. Dimovski, M. Moncecchi, M. Merlo, "Impact of energy communities on the distribution network: An Italian case study," in Sustainable Energy, Grids and Networks, Volume 35, 2023, 101148, ISSN 2352-4677, doi: 10.1016/j.segan.2023.101148.

[8] L. He and J. Zhang, "Energy trading in local electricity markets With behind-the-meter solar and energy storage," in IEEE Transactions on Energy Markets, Policy and Regulation, vol. 1, no. 2, pp. 107-117, June 2023, doi: 10.1109/TEMPR.2023.3250948

[9] T. Harighi, A. Borghetti, F. Napolitano and F. Tossani, "Optimization Model for the analysis of multiple energy communities in the same distribution network with different providers," 2023 IEEE Belgrade PowerTech, Belgrade, Serbia, 2023, pp. 1-6.

[10] D. P. Bertsekas and J. N. Tsitsiklis, "Parallel and distributed computation: numerical methods," Athena Scientific, 1997.

[11] J. Peschon, D. S. Piercy, W. F. Tinney, and O. J. Tveit, "Sensitivity in power systems," IEEE Trans. Power Appar. Syst., vol. PAS-87, no. 8, pp. 1687–1696, 1968.

[12] M. E. Baran and F. F. Wu, "Network reconfiguration in distribution systems for loss reduction and load balancing," in IEEE Trans. on Power Delivery, vol. 4, no. 2, pp. 1401-1407, April 1989, doi: 10.1109/61.25627.

[13] B. A. Robbins, H. Zhu and A. D. Domínguez-García, "Optimal tap setting of voltage regulation transformers in unbalanced distribution systems," in IEEE Trans. on Power Systems, vol. 31, no. 1, pp. 256-267, Jan. 2016, doi: 10.1109/TPWRS.2015.2392693.

[14] T. Harighi, A. Borghetti, F. Napolitano, F. Tossani, "Provision of reactive power services by energy communities in MV distribution networks," Sustainable Energy, Grids and Networks, Vol. 34, 2023, pp. 101038 1-15, doi: 10.1016/j.segan.2023.101038.

[15] Visual Crossing Weather. https://www.visualcrossing.com/

[16] Data available at the web address: https://www.doi.org/10.17632/8vzjxbxnnh